

Preparation and evaluation of biological activity of ZSM-5 nanoparticles loaded with gefitinib for the treatment of non-small cell lung carcinoma

Farah Al-Sahlawi^{1,2}, Israa Al-Ani¹, Mohamed El-Tanani¹, Hafiz Aadil Farooq³

¹ Faculty of Pharmacy, Pharmacological and Diagnostic Research Center, Al-Ahliyya Amman University, Amman, Jordan

² Faculty of Pharmaceutical Sciences, UCSI University, Kuala Lumpur 56000, Malaysia

³ Institute of Chemical Sciences, Bahauddin Zakariya University, Multan 60800, Pakistan

Corresponding author: Israa Al-Ani (ialani@ammanu.edu.jo)

Received 9 September 2023 ♦ Accepted 3 January 2024 ♦ Published 25 January 2024

Citation: Al-Sahlawi F, Al-Ani I, El-Tanani M, Farooq HA (2024) Preparation and evaluation of biological activity of ZSM-5 nanoparticles loaded with gefitinib for the treatment of non-small cell lung carcinoma. *Pharmacia* 71: 1–12. <https://doi.org/10.3897/pharmacia.71.e112449>

Abstract

Background: Gefitinib (GEF) is a tyrosine kinase inhibitor that has proven good efficacy against Non-small cell Lung Carcinoma (NSCLC). It has low solubility and dissolution rate and low oral bioavailability. This work aimed to improve efficacy by loading on ZSM-5 silica nanoparticles and testing the prepared delivery system on A-549 lung cancer cells.

Methods: ZSM-5 was synthesized in the laboratory and different methods of loading GEF on the nanoparticles were used, then the system was characterized by X-ray diffraction, Fourier Transform Infra-Red (FTIR), and drug release and dissolution.

Results and conclusion: GEF-loaded nanoparticles (NPs) showed prolonged release of GEF over 12 hours with an improved biological efficacy expressed by the decrease in IC₅₀ compared to free GEF ($P < 0.001$) using 3-[4,5-dimethylthiazol-2-yl]-2,5 diphenyl tetrazolium bromide (MTT) assay. Also, there was a significant decrease in migration and colony formation ability of the GEF-loaded NPs on A-549 lung cancer cells. In conclusion, loading GEF onto ZSM-5 NPs resulted in a lower IC₅₀ and improved biological action toward A-549 cells.

Keywords

ZSM-5, Gefitinib, Non-small lung cell carcinoma

Introduction

Throughout the world, lung cancer (LC) is a serious health issue. Each year, more than 1.6 million new cases of LC are identified. Every year, it accounts for over 1.4 million cancer deaths (Siegel et al. 2022). The most prevalent

form of LC in smokers, nonsmokers, and those under 45 is lung adenocarcinoma (Fois et al. 2021). About 30% of male smokers' original lung tumors and 40% of female smokers' first lung tumors are caused by adenocarcinoma. These percentages are close to 60% for men and 80% for women among non-smokers (Al-Najjar et al. 2022). Non-

small cell lung cancer (NSCLC) and small cell lung cancer (SCLC) are two major categories for treatment aims, and 80–85 percent of studies are for NSCLC (Jadus et al. 2012).

Tyrosine kinases regulate signaling cascades, deoxyribonucleic acid (DNA) repair, and programmed cell apoptosis, all of which are important for cell proliferation (Chemmalar et al. 2021). Tyrosine kinase inhibitors are used to treat several forms of cancer by blocking target cells' downstream signaling pathways as well as autophosphorylation (Amin et al. 2022). One of these is gefitinib (GEF), an oral tyrosine-kinase inhibitor used to treat metastatic NSCLC (Li et al. 2019). According to biopharmaceutical classification systems, GFT is class II because it has poor solubility and a low bioavailability of about 60% (Sherif et al. 2023), both of which reduce medicine efficacy and necessitate high drug doses. Unfavorable side effects include anorexia, diarrhea, vomiting, stomatitis, nausea, and hepatic dysfunction (El-Shenawy et al. 2023). Additionally, the clinically effective cure is limited by the majority of patient-acquired GEF resistance (Liao et al. 2022).

A number of experiments were conducted to improve the solubility and dissolution rates of GEF, such as the complex formation between GEF and cucurbit 8-urils, which demonstrated an enhanced GEF dissolution rate (Huang et al. 2014). Additionally, Godugu et al.'s creation of GEF-loaded controlled-release chitosan microparticles showed an improvement in the oral bioavailability of GEF (Golubeva et al. 2022). Srinivas et al. created NPs of Eudragit RL100 loaded with GEF, and they demonstrated an enhancement in the drug's bioavailability and dissolution (Srinivas et al. 2016).

Inorganic zeolite nanocarriers, which are a member of the aluminosilicate mineral family, have recently attracted attention as drug delivery systems in pharmaceutical research for several pharmaceutical medications (Yang et al. 2018). The SiO₄ and AlO₄ tetrahedral oxygen-sharing structures are the fundamental zeolite building blocks (Jesudoss et al. 2018). ZSM-5 is a nanocarrier with a highly ordered and distinguishable structure, a large surface area, a high thermal stability, a high shape selectivity, a high internal surface area with a big pore volume, and an acidic site (Amani et al. 2019). In the context of ZSM-5, "high shape selectivity" refers to its capacity to selectively let molecules with certain sizes or shapes to enter and interact inside its structure; this property makes ZSM-5 very useful for catalyzing processes involving molecules with dif-

ferent geometries. The ZSM-5 zeolite is reported to have two channel systems: a sinusoidal channel with 10-ring apertures of 5.4–5.6 Å and a straight channel with 10-ring openings of 5.1–5.5 Å. Zeolites are suitable for advanced medical technology because of these distinctive properties (Jiang et al. 2021). Drug delivery systems generally use a prolonged release strategy to prevent rapid breakdown and reduce drug toxicity (El-Sawi et al. 2021). Zeolite that has been loaded with medicines makes sparingly soluble compounds more soluble (Martinho et al. 2015) and the medication changes from a crystalline order structure to an amorphous, less crystalline structure when loaded in a porous zeolite nanocarrier. This happens when the drug crystals are solubilized and dispersed in the NPs pores or by the mechanical force that is applied in some methods of preparation that crushes the crystals and destroys the crystal lattice, thereby decrease the energy of solubilization. This will enhance its solubility and dissolution rate especially for hydrophobic drugs (Yang et al. 2018). The dimensions of ZSM-5 are shown in Fig. 1. The internal of pores could accommodate the drugs' molecules and the pattern of release depends on the number and strength of the binding forces created during the loading of the medication.

Zeolites, especially ZSM-5 can be employed as inorganic drug delivery systems. The system was utilized successfully to produce controlled release fluorouracil and 6-mercaptopurine (Jakubowski et al. 2022) and silver sulfadiazine (Mavrodinova et al. 2017),

For a number of reasons, sustained release formulations have the potential to increase the bioavailability of class 2 APIs like Gefitinib (GEF) (Zhai et al. 2022).

Maintaining Steady Drug Levels Despite Class 2 APIs' Poor Solubility and Permeability, They Always Work. Traditional immediate-release formulations cause a sharp increase and subsequent drop in plasma concentration because of the drug's quick absorption. Because of possible insufficient drug dissolution and gastrointestinal (GI) tract permeation time, this may reduce medication efficacy. The medication concentration in the blood is more reliably kept constant by sustained-release formulations, which release the drug slowly and consistently over time. This can improve class 2 active pharmaceutical ingredient (API) uptake (Pandit et al. 2022).

Peaks and valleys in drug concentration are lessened with sustained release formulations, which is particularly helpful for class 2 APIs with variable absorption. Improved

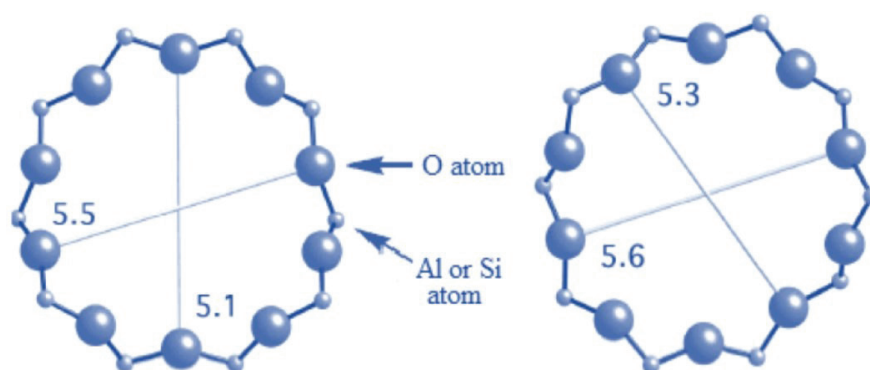


Figure 1. Ring structures and main channel dimensions in ZSM-5 (Alnaama, 2015).

medication exposure and effectiveness as well as decreased risk of adverse effects due to dosing variations are all possible with prolonged-release formulations (Salehi et al. 2021).

As a result of the drug's gradual release, class 2 APIs like Gefitinib have more time to break down and be absorbed from the GI tract's absorptive surfaces. This is especially helpful for medications that don't dissolve well in water (Elzayat et al. 2023).

Increased adherence is especially important for patients using oral medicines. Dosing intervals for sustained-release formulations are often longer than those for quick-release formulations. This may improve patient compliance with the treatment plan, which in turn increases the class 2 API's bioavailability (Johnie et al. 2020).

Some class 2 APIs have their bioavailability drastically lowered due to extensive first-pass metabolism in the liver. The steady release of the medication over time in sustained release formulations reduces the amount of first-pass metabolism, so that more of the drug reaches the systemic circulation without being broken down by the liver (Huang et al. 2022).

It is less likely that the gastrointestinal mucosa will be irritated by the medicine, which is important since certain class 2 APIs may irritate the mucosa and cause side effects that may reduce drug absorption. Sustained-release formulations, which gradually release the medicine into the body, may assist alleviate this problem by lowering the peak drug concentration in the digestive system (Shah et al. 2021).

Sustained release formulations have the potential to increase the therapeutic impact while decreasing the likelihood of either hazardous or subtherapeutic medication concentrations by keeping drug levels within a tighter, ideal therapeutic window (Malam et al. 2009).

Depending on the drug's physicochemical qualities and pharmacokinetics, not all class 2 APIs will gain the same advantages from sustained-release formulations. The efficacy of sustained-release formulations for a given API is generally evaluated via formulation development and bioequivalence studies. Bioavailability and therapeutic effects may be improved by striking a good balance between the release rate and absorption properties (Cheng et al. 2020).

Zhao et al. (2021) creatively created a unique ZSM-5/ZIF-8 miR-34a formulation to promote RNA regulation treatment (Abd El Azeem et al. 2019). The production of the nanocarrier, which successfully loaded miR-34a in ZIF-8 and ZSM-5, greatly increased the effectiveness of miRNA delivery to target cells. As a result, the expression of the Bcl-2 gene was inhibited, which increased the cellular cytotoxicity against cancer cells. This exciting development highlights ZSM-5/ZIF-8's potential as a powerful platform for RNA-based therapy optimization.

The aim of this study was to achieve a regulated release of GEF, enhancement of solubility, and improve its pharmacological efficacy through its encapsulation in ZSM-5 NPs and evaluation of this suggested delivery system.

The drug release and the cytotoxic activity of the loaded drug samples were assessed in comparison to the native GEF. The interactions between the GEF and the host and the properties of the ZSM-5 surface were to be used to explain

the findings. To our knowledge, this is the first time ZSM-5 nanoparticles have ever been used to encapsulate GEF.

Materials and methods

Materials and instruments

Chemicals for analysis and synthesis were as follows: Gefitinib (GEF) (Tokyo Chemical Industrial/Japan), Dimethylsulfoxide (DMSO) (ChemCruz/USA), Dulbecco's phosphate-buffered saline (Euro-Clone S.p.A/Italy), Trypsin-EDTA 1X in PBS (Euro-Clone S.p.A/Italy), Formic acid (Sigma-Aldrich/China), Methanol (Sigma-Aldrich/France), MTT [3-(4,5-Dimethylthiazol-2-yl)] (Thermo-Fisher Scientific/USA), Penicillin-Streptomycin Solution (Euro-Clone S.p.A/Italy), Tetrapropylammonium hydroxide, Tetraethyl orthosilicate, and Trifluoroacetic acid (Sigma-Aldrich), Tween 80 (Janssen Chemica/USA). And the Chemicals for nanoparticle synthesis were: Tetrapropylammonium hydroxide, Sodium hydroxide, Aluminum sulfate anhydrous.

Method of analysis of GEF by HPLC

High-performance liquid chromatography with LC solution software (Model: KMC-130SH) (Shimadzu/ Japan) was used to analyze GEF. The Mobile phase of the analysis of GEF is composed of (Trifluoroacetic acid Orthophosphoric acid mixture each 0.1% in deionized water): methanol (1:1). The column used was EC 250/4.6 Nuclerdur 100 C18 at temperature (30 °C). The injection volume was 10 µl, the flow rate was 1 ml/min, and lambda max was set at 246 nm (Faivre et al. 2011). The linearity and calibration curve was obtained in the range of 5–30 µg/ml range. Serial dilutions were made from a stock solution of 1000 µg/ml in methanol using the mobile phase. Regression and R² were calculated using the software of the instrument.

Preparation of ZSM-5 NPs

The synthesis of ZSM-5 nanoparticles was prepared as follows: 12.5 g of tetrapropylammonium hydroxide was dissolved in 50 mL of deionized water. Then 12.0 g of tetraethyl orthosilicate was added dropwise to the reaction flask at room temperature. The flask was placed in a water bath with vigorous shaking for 24 hours at 80 °C. In a separate flask, 0.24 g sodium hydroxide and 0.722 g aluminum sulfate anhydrous were mixed in 4 ml deionized water and poured into the previous mixture. The mixture was placed in acid digestion vessels for forty-eight hours at 170 °C. Finally, the obtained nanoparticles were washed twice with distilled water, filtrated, and calcined in a furnace for 6 hours at 500 °C (Anaya et al. 2022).

Loading of GEF on ZSM-5 NPs

GEF was loaded onto the prepared ZSM-5 nanoparticles using solvent evaporation, kneading, adsorption, and physical dry mixing (El-Sawi et al. 2021). In all methods,

the ratio of drug to carrier was 1:1 w/w. Then the method that gave the highest percent loading was followed in the preparation of 1:2 and 1:3 w/w to investigate the efficacy ratio of drug carriers on the loading efficacy of the drug.

In the solvent evaporation method, 0.05g of GEF was dissolved in 15 mL of methanol, and then, in a conical flask, 0.05 g of ZSM-5 was added. The rationale for using methanol as the solvent is its capacity to effectively dissolve GEF and provide a uniform combination with ZSM-5. Drug-loaded nanoparticles are left behind because methanol's volatile nature makes evaporation simple. Materials that dissolve easily in organic solvents may be used using this technique. The mixture was kept for 24 hours with continuous stirring at 40 rpm at room temperature. Then the heat was applied (40 °C) for 24 hours at the same stirring rate to evaporate the solvent. Then the sample was transferred to a container and kept in the desiccator.

For the kneading method, 0.05 g of each GEF and ZSM-5 were weighted and mixed in a porcelain mortar. The vehicle was prepared from methanol and phosphate buffer in a ratio of 1:1 (pH 3). The kneading process uses a pH 3 combination of phosphate buffer and methanol. This mixture is chosen to make a paste that will distribute GEF and ZSM-5 uniformly. Methanol helps to generate a paste for uniform drug and carrier integration, and the pH of 3 is used to preserve the stability of GEF throughout production. The solvent was added drop by drop until a paste was formed. Trituration was continued for one hour; then, the sample was kept in an oven at 40 °C for 24 hours for drying. The powder was sieved through a 0.305-mm mesh and kept in the desiccator until used.

Physical mixing used the same procedure as kneading but without solvent. Direct blending of GEF with ZSM-5 requires just dry mixing, which is accomplished physically without the need for a solvent. This approach simplifies the loading procedure by removing the need for a solvent during the drug's integration with the carrier. Dry mixing was achieved for one hour manually. The sample was sieved and kept in the desiccator until used.

In the adsorption method, 0.01g of GEF was mixed with 0.01 g of ZSM-5 and 25 ml of distilled water. To take use of the hydrophilic properties of ZSM-5, distilled water is used as the solvent in the adsorption process. Water ensures that the medication and carrier are stable by facilitating the adsorption of GEF onto the nanoparticles without the need for organic solvents. The mixture was stirred for 24 hours at 40 rpm and filtered using filter paper. The powder was centrifugated at 4000 rpm for 5 minutes and then dried.

The kneading method was performed using different ratios of GEF to the carrier. 1:1, 1:2, and 1:3 ratios were prepared using the same procedure to investigate the effect of the drug-to-carrier ratio on the loading efficiency of GEF.

Characterization of the unloaded and loaded NPs

The FTIR spectrum for ZSM-5 was recorded over the range 400–4000 cm⁻¹. The samples were analyzed using

the Fourier infrared spectrophotometer (IR Prestige-21, Shimadzu Europa GmbH) using the KBr disc. IRsolution FTIR control software supports FDA 21 CFR Part 11 compliance and provides a resolution of 2 cm⁻¹. GEF, unloaded ZSM-5 NPs and the loaded NPs were investigated.

The XRD patterns were acquired using an X-ray diffractometer (Shimadzu XRD-7000, Japan) equipped with a CuK radiation source and a Ni filter operating at 40 kV/30 mA in the range 2° ≤ 60°. The scanning speed was 2° per minute, and the sampling pitch was 0.02°. The obtained PXRD data were analyzed with the X'Pert HighScore Plus 2.2 software using search-match operations to completely identify the inorganic crystal structure. Also, GEF, unloaded ZSM-5 NPs and the loaded NPs were investigated.

To record the SEM of the loaded ZSM-5 nanoparticles, a sample piece was transferred into an adhesive carbon and cleaned with N₂ gas. The morphology and chemical composition of samples were investigated by a Phenom XL G2 scanning electron microscope (Thermo Fisher Scientific) coupled with an AXS EDS system. The SEM images were collected at 0.06–0.04 mbar with a 15 kV accelerating voltage. BET samples were recorded using an N₂ adsorption-desorption analyzer (Autosorb IQ, Quantachrome Instruments version 5.21, Boynton Beach, FL, USA).

For pH measurement, 100 mg of the prepared loaded NPs were suspended in 100 mL of distilled water, and the pH of the solution was measured by a pH meter. Also, the NPs size was measured by Zetasizer (Malvern, Worcestershire, UK). The nanoparticles sample of 10 mg was suspended in 10 mL of deionized water, and the suspension was diluted 125-fold using deionized water before measurement.

Percent GEF loaded on ZSM-5 NPs was measured by suspension of 0.05g of the loaded GEF nanoparticle powder in 25mL methanol with sonication to extract the drug completely from the nanoparticles. The solution was filtered and diluted with a solvent composed of (35:65 acetate buffer: methanol) pH 3, and the concentration of GEF was measured using the developed HPLC analysis method. Percentage drugs loaded on the NPs was calculated using the following equation (Martinho et al. 2015):

$$\% \text{Drug loading} = \frac{\text{(Weight of drug in nanoparticles)}}{\text{(Weight of nanoparticles)}} \times 100\%$$

Characterization of the crystalline structure of the loaded NP was done using X-ray diffraction, and FTIR investigated the detection of binding of the drug to the carrier. The spectrum of free GEF and GEF-loaded NPs were taken, and results were compared with the free carrier.

GEF release from ZSM-5 NPs

GEF release from the loaded nanoparticle was studied using USP apparatus II in phosphate buffer pH 6.8 (Yang et al. 2018). The dissolution conditions were set: dissolution medium phosphate buffer with pH 6.8, temperature

37 °C, stirring speed 50 rpm. Due to the sensitivity of GEF to light, the whole apparatus and all equipment were wrapped in aluminum foil. 50 mg of pure GEF powder and ZSM-5-GEF loaded using the kneading method (1:1 w/w equivalent to 50 mg GEF) were put in each jar at time zero, and the test was run for 60 min. 5 mL of the sample was withdrawn and replaced by fresh media at the following times: 5, 10, 20, 30, 45, 60, and 70 minutes, and diluted with the mobile phase. Its concentrations were measured using HPLC. The same procedure was repeated for GEF pure powder.

Since pH 6.8 is often used to simulate the gut pH in release experiments, it is possible that the formulations were intended for oral delivery. The small intestine is often where medication absorption occurs, and its pH range is 6.8. It is crucial to examine release profiles at various pH settings, including the stomach's acidic environment (pH 1.2), considering the thorough assessment of drug release.

Based on the result of the test, the release test was repeated for 12 hours. The same amount of the loaded NPs was used in each of the 6 jars to perform the test and the same conditions were used. Samples were withdrawn at 20 min, 40 min to detect any possible burst effect, Then 1, 2, 3, 4, 6, 8, 10, and 12 hours.

Biological assay of ZSM-5- GEF loaded nanoparticle

IC50 determination

IC50 was determined using the MTT Cell Proliferation Assay as follows: In a 96-well plate, 10,000 cells of the A-549

cell line were cultured in 100 l of DMEM medium in each well, and then the plate was placed in a CO₂-incubator at 37 °C for 24 hours. After removing the medium from the wells, different doses (i.e., 100 nM, 200 nM, 300 nM, 500 nM, and 700 nM) of GEF, ZSM-5, GEF-ZSM-5 loaded nanoparticles (prepared by the kneading method), and DMSO (as a negative control) were prepared in 100 l medium and added to the wells. The plate was incubated in a humidified 5 percent CO₂ incubator at 37 °C for 4 hours. Next, 85 l of medium was discharged from each well, and 50 l of DMSO was added. Then, after 10 minutes, the absorbance was recorded at 590nm using a Biotech 96-well plate reader. Finally, the IC₅₀ value was determined using Prism-GraphPad.

Migration test

In this test, 250,000 cells of A-549 were seeded in each well of a 12-well plate in 2 mL DMEM medium and incubated at 37 °C in 5% CO₂ and 95% humidity for 24 hours. A straight-line scratch from the top to the end of each well was produced using a sterile tip, then the media was discarded and the cells were washed using phosphate buffered saline (PBS). After that, 1 mL of media was added to each well, and each of the three wells was treated using 0.5 IC₅₀, IC₅₀, and 2 IC₅₀ of the ZSM-5-GEF-loaded nanoparticle. Up to 2 mL of media was added to each well. DMSO and media were used as controls. A photo was taken using a Nikon camera on days one and two, and the area of migration was measured using Motic Images Plus version 2.0; finally, the motic area was calculated using the equation below (Haggag et al. 2022).

$$\text{Motic area} = \frac{\text{Area of scratch measured immediately after scratching} - \text{area measured after 24 hours}}{\text{Area of scratch measured immediately after scratching}} \times 100$$

Colony formation assay

In a 12-well plate, 200 cells of A-549 were seeded in 2 mL of medium in each well and incubated for 24 hours in a 5% CO₂ incubator at 37 °C. After 24 hours, the media in each well were replaced with 1 mL fresh media, and the cells in 3 wells were treated using 0.5 IC₅₀, IC₅₀, and 2 IC₅₀ of free GEF, respectively. While the cells in the other three wells were treated using 0.5 IC₅₀, IC₅₀, and 2 IC₅₀ of loaded GEF. DMSO and media were used as controls. After that, up to 2 mL of media was added to each well. Then the plate was incubated in a 5% CO₂ incubator at 37 °C for seven days. After seven days, the colonies in each well were counted and recorded.

Statistical analysis

All statistical analysis results were performed using GraphPad Prism 8 via Two-way ANOVA. The results were presented as mean ± SD. Statistical significance was represented as *P < 0.05, **P < 0.01, and ***P < 0.001.

Results and discussion

Development of method of analysis of gefitinib by HPLC

HPLC was used to determine how much gefitinib is contained inside the nanoparticles and how much medicine will be released. At a retention time (RT) of 1.626 minutes, a peak corresponding to GEF was seen. The peak was sharp and highly resolved. Pure GEF concentrations were measured and used to create the calibration curve shown in Fig. 2. The R² value for linearity was 0.99999.

Synthesis ZSM-5 nanoparticle

No deviations from the method described by Hodali and Marzouqa (Hodali & Marzouqa, 2016) were made during the synthesis of ZSM-5 nanoparticles. Drying for 4 hours at 100 degrees Celsius was more than enough time to ensure a well dried out final product. When heated to 500 degrees Celsius for 24 hours, the

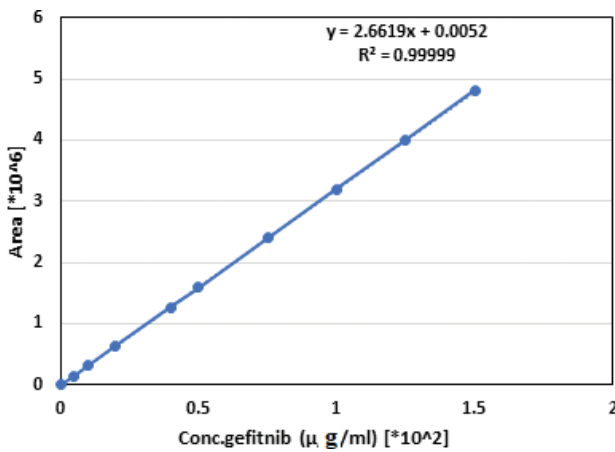


Figure 2. Linear regression and calibration curve of GEF.

material is reduced to a white powder. The finished powder was then stored in a desiccator, away from any possibility of dampness.

Characterization of the unloaded and loaded NPs

For the FTIR analysis, the spectra shown in Fig. 3A shows the characteristic peaks of stretching vibration for GEF: C-Cl at 800 cm⁻¹, C-F at 1028 cm⁻¹, C-O at 1110 cm⁻¹, C=C (Aryl) at 1500 cm⁻¹, and N-H at 3400 cm⁻¹. For the ZSM-5 (Fig. 3B), while Fig. 3C shows the spectrum of the ZSM-5 NPs loaded with GEF. The characteristic peaks were detected: tetrahedron internal vibration at 540 cm⁻¹, S-O stretching

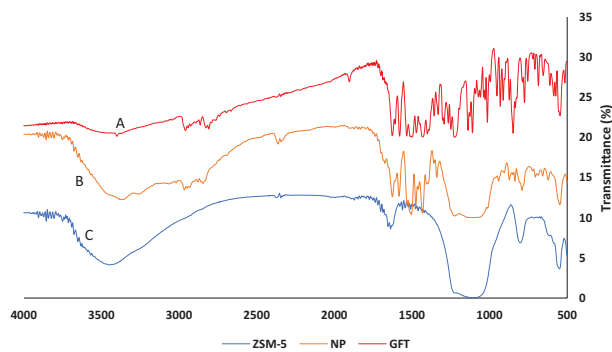


Figure 3. FTIR data of (A) GFT, (B) ZSM-5 loaded nanoparticles and (C) ZSM-5 NP.

at 620 cm⁻¹, Si-O-Si symmetry stretch at 800 cm⁻¹, Si-O-Si asymmetric stretching at 1099 cm⁻¹, and Si-OH-Stretch at 3360 cm⁻¹. These results agreed with (Cheng et al. 2017).

The results clearly depict changes to representative GEF peaks in the spectrum of the loaded carrier vibration. The carbonyl peak (C=C, C=N) at the higher frequency indicates intermolecular interactions between the GEF and the ZSM-5 nanocarriers. The O-H of the nanocarrier is overlaid with the N-H peaks of the GEF in the spectrum. Hydrogen bonding interactions between hydrogen donor ZSM-5 and hydrogen receiver GEF may have contributed to the observed results. Furthermore, there were a lot of hydrophobic interactions between the carbon rings, the surface zeolite, and the bridging oxygen. The same hypothesis was supported by a recent study by Narayan et al. that showed favorable interactions between the MCM-41 surface and the antibiotic 5-fluorouracil through hydrogen bond donors and acceptors (Narayan et al. 2022).

The XRD spectrum of ZSM-5 (Fig. 4A) reveals FTIR data of GFT, ZSM-5 loaded nanoparticles and ZSM-5NP GFT shows fluctuations adversely at initial stage varying from 28–30°. It abruptly goes up at 1700 and then slowly comes down and shows little variations. NP shows variation not much similar to ZSM-5 but smooth fluctuations and goes up at 1700 slowly comes down at 2700 then goes up at 3700 and gains constant. ZSM-5 shows little fluctuations comes down at 1000 gains height of 1500, very little fluctuates and goes up, slightly comes down at 3500 and then again gain heights. The same pattern was reported by (Cheng et al. 2017). At the same time, the crystal structure of pure GEF (Fig. 4B) with sharp peaks at 18.6°, 19.2°, 24.2°, 26.2°, and 26.4° has been reported as shown in Fig. 4C.

Drug encapsulation into the nano carrier ZSM-5 is the cause of the sharp two peaks at 18.6 and 19.2 of crystalline GEF disappearing from the drug-loaded ZSM-5 diffractogram, while the fundamental peaks of ZSM-5 are retained and have minimal peak strength. It is noteworthy that the presence of GEF in the amorphous phase may increase GEF's solubility and dissolution rate, which are responsible for the lowering of the peaks of loaded ZSM-5. These findings support the Zarshenas groups' observation that the XRD pattern of 5-fluorouracil-loaded ZSM-5 demonstrates full encapsulation within ZSM-5 and the absence of loose crystalline 5-fluorouracil (Zarshenas et al. 2022).

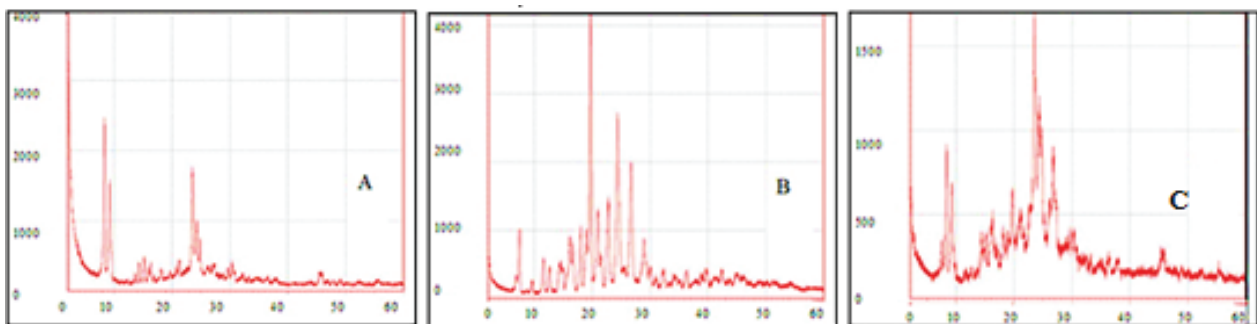


Figure 4. X-ray diffraction pattern of (A) ZSM-5, (B) GFT and (C) ZSM-5 loaded GFT nanoparticles.

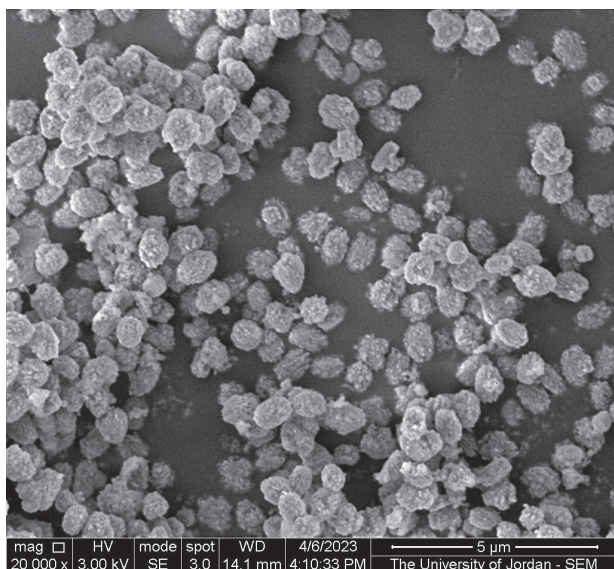


Figure 5. SEM photo of the prepared ZSM-5 nanoparticles

Scanning Electron Microscope (SEM) photo shows the morphology of the prepared NPs (Fig. 5). The result confirms the formation of ZSM-5 zeolite (Shi et al. 2018).

Fig. 5 shows properties of nanoparticles of ZSM-5. Its size is 5µm, 14.1mm wide and HV is 3.00kv. the same shape was obtained with (Sun et al. 2020).

The pH of the ZSM-5 nanoparticle suspension was 7.71 ± 0.05 , close to the pH of biological fluids. (Trumer et al. 2012) reported the pKa of GEF 5–7, which means the above pH 7 GEF mostly exists in its unionized form which is the biologically favored species.

The average particle size of the ZSM-5 NPs was between 100–200 nm, with a polydispersity index (PDI) equal to 0.265 (Fig. 6). This range of particle size ranged from 100 to 200 nm, which satisfies the criteria for nanoscale drug delivery systems that provide a high surface area per unit weight of the system with good safety (Kariminezhad et al. 2015)

The percent yield of the NPs and loading efficiency of GEF are represented in Table 1. Results showed the highest loading efficiency was obtained with the kneading method with no effect of the drug to the NPs ratio on the percent loading. Physical adsorption and physical mixing methods gave less than the kneading method with

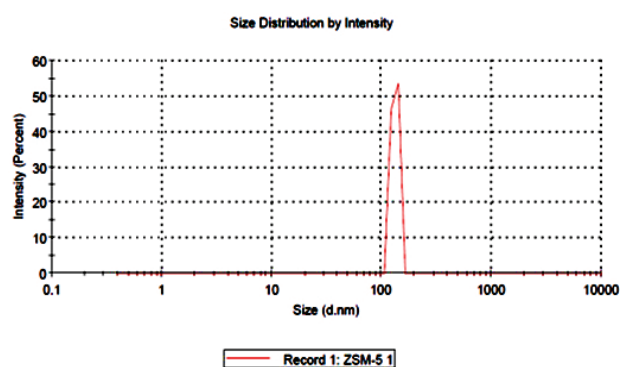


Figure 6. Particle size distribution of the prepared ZSM-5-GFT nanoparticles.

Table 1. Percent yield and loading efficiency of the prepared NPs.

Nanocarriers	% Percent yield	Loading efficiency
Physical adsorption method	60%	22%
Kneading method 1:1	75%	80%
Kneading method 1:2	73.3%	80%
Kneading method 1:3	75%	80%
Physical Mixing method	60%	79%
Solvent evaporation method	50%	76%

no differences between them. The method with the least efficiency was the solvent evaporation method.

The kneading procedure has the highest loading effectiveness (80%). However, physical mixing produced an extremely close result (79%). These two techniques are mixed with force. This technique works well for inserting medications into zeolite nanoparticles. In this procedure, a known volume of a concentrated medication solution is employed that is roughly equivalent to the nanocarrier's pore volume. The medication then diffuses into the pores as a result of capillary action. Additionally, this technique demonstrated how many impregnations could fill pores and improve drug loading concentration. The kneading approach is more effective than the other conventional loading processes, according to our research. The key benefits of the kneading method include high loading capacity, minimal solvent use, and suitability for expensive drugs. As a result, the ratio of drug to carrier had little effect on loading efficiency, implying that the pores were almost filled with drug. This result is consistent with that of the work by (Charnay et al. 2004).

Samples prepared by kneading method in the ratio of 1:1 were chosen to complete the studies.

GEF release from NPs

The GEF release from the loaded ZSM-5NPs is represented in the dissolution profile shown in Fig. 7. Results showed a significant difference in percent drug release at 5 minutes of $20\% \pm 3.5\%$ of loaded GEF versus $68\% \pm 1.8\%$ of free drug and $35\% \pm 2.6\%$ of loaded NPs versus $70\% \pm 3.0\%$ in 60 minutes and all these differences were significant using 5% as a confidence interval. These results suggested the prolonged release of GEF from the NPs.

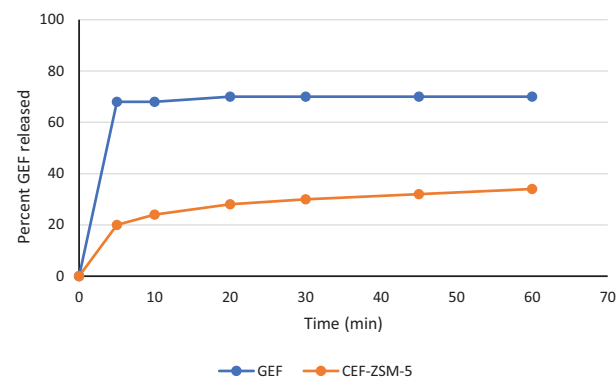


Figure 7. Drug release profile of free GEF and GEF from the loaded NPs for 60 min, phosphate buffer pH 6.8, apparatus II (paddle), 50 rpm, and 37 °C.

The results of the dissolution test for 12 hours are represented in Fig. 8. This result supported the prolonged release pattern with zero-order release over time 1–12 hrs with a correlation coefficient R2 equal to 0.993.

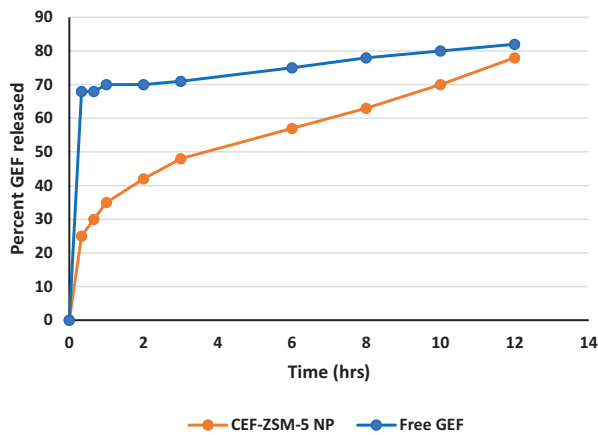


Figure 8. Drug release profile of free GEF and GEF from the loaded NPs for 12 hr, phosphate buffer pH 6.8, apparatus II (paddle), 50 rpm, and 37 °C.

The typical profiles of release obtained from ZSM-5 nanoparticles may be caused by diffusion through the ZSM-5 nanoparticle, transport through water-filled pores, or the initial high release. It also has to do with the process of interfacial diffusion between the solid surface nanoparticle and the dissolution medium. In the latter scenario, the release rate is thought to be proportional to the difference between the drug concentration at the time of analysis in the phosphate buffer media and the drug concentration in the core of the nanocarrier (Godugu et al. 2015). In comparison to the free drug, the loaded GEF was released slowly over a 60-minute, with 35% of the loaded drug being released. When performing the test for 12 hours, the slow release of GEF followed a zero-order pattern with a correlation of 0.999 between 1–12 hrs with a total 80% of drug release. Armando et al. suggested these mechanisms in their research. Since the free drug gave 68% dissolution in the first 5 min, the sink condition was mostly achieved, and the NPs might be a good candidate for prolonged action.

GEF from the loaded NPs dissolves much more slowly than pure GEF. This is as a result of the GEF's regulated release made possible by the NPs. Just 20% of the GEF from the loaded NPs had dissolved after an hour, compared to 50% of the pure GEF. Only 30% of the GEF from the loaded NPs had dissolved after two hours, compared to 70% of the pure GEF. Over the time of study, the GEF from NPs release showed an almost zero-order controlled pattern of release.

There are several reasons why this regulated release of GEF may be advantageous. First, it may contribute to the body's ability to retain a steady level of GEF, which may result in more successful therapy. Because the medication is not delivered all at once, it may also lower the chance of adverse effects. Thirdly, since the medication doesn't need to be taken as often, it may increase patient compliance.

All things considered, the dissolution profile of both pure GEF and GEF from the loaded NPs demonstrates that the NPs provide a regulated release of the medication. Improved patient compliance, a lower chance of adverse effects, and more effective therapy are just a few advantages of this.

Biological assay of ZSM-5-GEF loaded NPs

Results of the MTT assay, colony formation, and migration assays are shown in Fig. 9. The viability assays revealed that blank (media) and control (media) had no apparent toxicity on A549 cells. The IC₅₀ for free GEF was 704.1 nM, while the IC₅₀ for GEF-ZSM-5 loaded was 518 nM. A significant decrease ($P = 0.00069$) in IC₅₀ between free GEF and loaded GEF on ZSM-5 NPs. The normalization of the transform of carrier only, free GEF, and GEF-ZSM-5 loaded using the kneading method is seen in Fig. 10.

Comparing our prepared blank ZSM-5 nanoparticle to the drug-loaded ZSM-5 nanoparticle, the cellular studies showed that our prepared blank ZSM-5 nanoparticle is safe and biocompatible. The GEF medication had an IC₅₀ of 704.1 nM compared to 518 nM for the GEF-loaded ZSM-5 nanoparticle in the cell viability MTT experiment. Intriguingly, as shown in Fig. 9 (Kutkut et al. 2023), GEF-loaded ZSM-5 nanoparticles demonstrated greater cytotoxicity compared to the original medication after 24 hours of therapy.

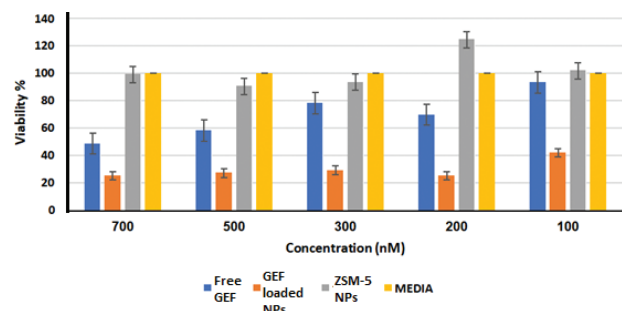


Figure 9. Viability percent for free GEF, GEF-loaded NPs, ZSM-5 NPs, and media (DMSO).

The innovative GEF encapsulation using ZSM-5 increased antitumor activity as an appropriate drug delivery mechanism, which was confirmed by the MTT results. Additionally, ZSM-5 nanoparticles frequently cover up a drug's undesirable side effects and may enhance their pharmacokinetics and bioavailability (Haeri et al. 2014).

Due to differences in cellular processes uptake compared to the free pharmaceuticals, incubation for 24 hours might not provide the drug-loaded ZSM-5 nanoparticle with the best effect time (Zaleskis et al. 2021).

For the migration test, GEF does not significantly affect cells' migration. Fig. 11 shows The motic area was slightly higher in loaded GEF than in free GEF, but that difference was insignificant. Therefore, the pure GEF and GEF-ZSM-5 loaded using the kneading method of 1:1 w/w did not affect the cell migration (Tables 2, 3).

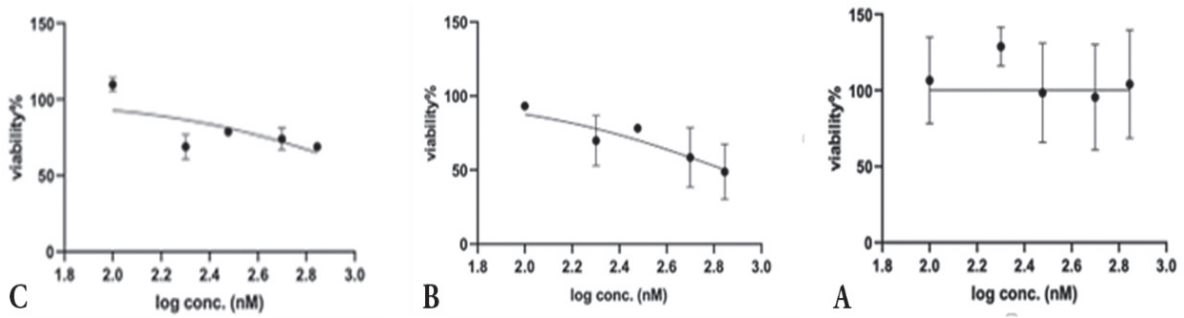


Figure 10. Normalized transform of A. ZSM-5 Carrier only; B. Free GEF, and C. GEF-ZSM-5 loaded prepared by kneading method (ratio 1:1).

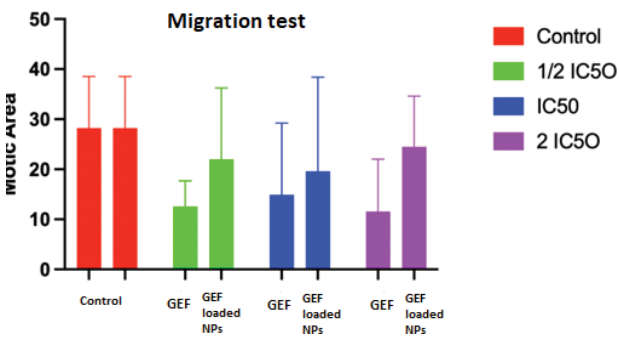


Figure 11. Control migration testing Treatment of A-549 cells with: Half-Maximal Inhibitory Concentration (IC50), IC50, 2 IC50, Double-Maximal.

Table 2. Closure % in the migration assay (media and free GFT).

Sample	Concentration	Day 1	Day 2	% closure
Control	Media			38.54%
Free GFT	1/2 IC50			17.7%
	IC50			10.55%
	2IC50			0.68%

A colony assay was used to study the growth rate of A-549 cells after treatment and the effect of proliferation without a drug. The average number of colonies was noticed, and growth was recorded according to the treatment plan after 13 days of seeding. Fig. 12 shows an insignificant decrease in cells treated using the IC50 of free GEF at the 0.05 CI level but a significant (**P 0.001) difference compared to control cells. While in A-549 cells treated using ZSM-5-GEF-loaded using the kneading method 1:1

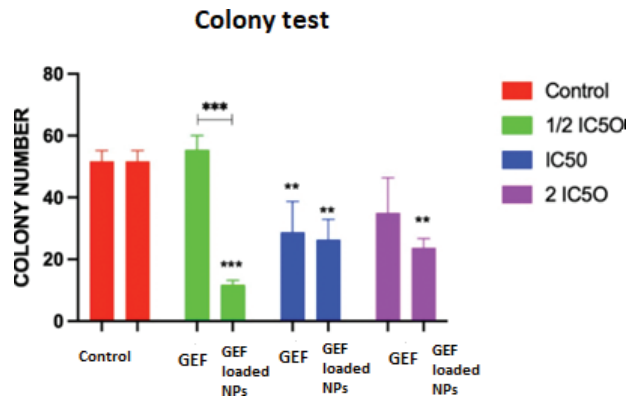


Figure 12. Colony test of untreated A-549 cells in a control. utilizing free gefitinib and ZSM- 5-gefitinib-loaded utilizing kneading technique 1:1 w/w, 12 IC50 stands for half dosage of the half maximum inhibitory concentration, IC50 for the half maximum inhibitory concentration, and 2 IC50 for double dose of the half maximum inhibitory concentration. Comparisons between each dosage and the control were made. The findings were shown as mean SD. The signs for statistical significance were *P 0.05, **P 0.01, and ***P 0.001.

Table 3. Closure % in the migration assay (ZSM-5 loaded GFT).

Sample	Concentration	Day 1	Day 2	% closure
ZSM-5-GEF-loaded	1/2 IC50			23.7%
	IC50			21.58%
	2IC50			14.34%

w/w, a significant decrease (**P 0.001, *P 0.01, **P 0.01 is seen in cells treated using 12 IC50, IC50, and 2 IC50, respectively, but not significant at the 0.05 level.

The results of the closure assay show that the drug-loaded ZSM-5 nanoparticle continues to act after 48 hours. The closure rate was significantly slower for drug-loaded ZSM-5 nanoparticles than for free

drugs, showing that GEF-loaded ZSM-5 nanoparticles were more effective at inhibiting cancer cell migration than free GEF drugs as a result of the new formulation's improved physicochemical properties and increased cytotoxicity effect on A549 cell lines. After treating A549 cell lines with IC₅₀ and 2 IC₅₀ concentrations and comparing the free drug with a drug-loaded ZSM-5 nanoparticle, the best closure percentage and meaningful results were obtained. By using these doses, a GEF drug-loaded ZSM-5 nanoparticle completely stopped cell migration with nearly no closure percentage. These findings verified the higher cytotoxicity of GEF-loaded ZSM-5 nanoparticles against A549 cell lines to suppress lung cancer metastasis and validated the MTT findings (Smith et al. 2017).

Additionally, the colony formation assays (Fig. 12) demonstrated the efficiency of GEF-loaded ZSM-5 nanoparticles by showing that no colonies formed over a 13-day treatment period. Even though the number of colonies counted in the two cells treated with either of the free medications was comparable to the number of colonies loaded with drugs in ZSM-5 nanoparticles, after 13 days, both free GEF and GEF-laden ZSM-5 nanoparticles showed a significant decline in colony formation. The potent novel formulation encapsulating medication against the A549 cell line (El-Tanani et al. 2022) may be to blame for this.

References

- Al-Najjar LM, Zihlif M, Jarrar Y (2022) Differential molecular alterations promoting non-small cell lung cancer under hypoxia. *Genome Instability & Disease* 3(2): 108–121. <https://doi.org/10.1007/s42764-022-00062-5>
- Amani S, Bagheri Garmarudi A, Rahmani N, Khanmohammadi M (2019) The β -cyclodextrin-modified nanosized ZSM-5 zeolite as a carrier for curcumin. *RSC Advances* 9(55): 32348–32356. <https://doi.org/10.1039/c9ra04739e>
- Amin H, Osman SK, Mohammed AM, Zayed G (2023) Gefitinib-loaded starch nanoparticles for battling lung cancer: Optimization by full factorial design and in vitro cytotoxicity evaluation. *Saudi Pharmaceutical Journal: SPJ: The Official Publication of the Saudi Pharmaceutical Society* 31(1): 29–54. <https://doi.org/10.1016/j.jsps.2022.11.004>
- Anaya H, Muhana F, El-Tanania M, Madi R, Kerfan R (2022) Mebendazole loaded nanoparticles for lung cancer therapy. *International Journal of Drug Delivery Technology* 12(03): 1053–1065. <https://doi.org/10.25258/ijddt.12.3.22>
- Charnay C, Bégu S, Tourné-Péteilh C, Nicole L, Lerner DA, Devoisselle JM (2004) Inclusion of ibuprofen in mesoporous templated silica: drug loading and release property. *European Journal of Pharmaceutics and Biopharmaceutics: Official Journal of Arbeitsgemeinschaft Für Pharmazeutische Verfahrenstechnik e.V* 57(3): 533–540. <https://doi.org/10.1016/j.ejpb.2003.12.007>
- Chemmalar S, Intan-Shameha AR, Abdullah CAC, Ab Razak NA, Yusof LM, Ajat M, Gowthaman NSK, Bakar MZA (2021) Synthesis

Conclusions

GEF was encapsulated in ZSM-5 NPs using the kneading method successfully with superior loading efficiency. The proposed delivery system showed prolonged release of GEF following zero-order kinetics of release for 12 hours which might be of noticeable advantage in decreasing side effects of the drug. Beside the statically improved efficiency against A549 cell lines, expressed by decreased IC₅₀ using MTT assay accompanied by significant decrease in colony formation for 13 days in colony formation test, the results suggested a promising delivery system for GEF for treating NSCLC patients.

Author contribution

All authors contributed to the study conception and design. All authors contributed to the material preparation and data collection and writing the manuscript. All authors read and approved the final manuscript.

Acknowledgments

The authors are thankful to the staff of Pharmacological and Diagnostic Research Center (PDRC) in Al-Ahliyya Amman University.

- and characterization of gefitinib and paclitaxel mono and dual drug-loaded blood cockle shells (*Anadara granosa*)-derived Aragonite CaCO₃ nanoparticles. *Nanomaterials (Basel, Switzerland)* 11(8): 1988. <https://doi.org/10.3390/nano11081988>
- Cheng M, Yu X, Lu K, Xie L, Wang L, Meng F, Han X, Chen X, Liu J, Xiong Y, Jin J (2020) Discovery of potent and selective epidermal growth factor receptor (EGFR) bifunctional Small-Molecule degraders. *Journal of Medicinal Chemistry* 63(3): 1216–1232. <https://doi.org/10.1021/acs.jmedchem.9b01566>
- Cheng Y, Wang L-J, Li J-S, Yang Y-C, Sun X-Y (2017) Preparation and characterization of nanosized ZSM-5 zeolites in the absence of organic template. *Materials Letters* 59(27): 3427–3430. <https://doi.org/10.1016/j.matlet.2005.06.008>
- El-Sawi SA, Motawae H M, Abdelkawy MA, Fekry MI, Youssef HF, Farghaly AA, Maamoun MAI (2021) Novel anticancer drug delivery system based on zeolite encapsulating hamelia patens leaf and flower extracts. *Indian Journal of Natural Products and Resources* 12(2): 181–194. <https://doi.org/10.56042/ijnpr.v12i2.22436>
- El-Shenawy AA, Elsayed MMA, Atwa GMK, Abourehab MAS, Mohamed MS, Ghoneim MM, Mahmoud RA, Sabry SA, Anwar W, El-Sherbiny M, Hassan YA, Belal A, Ramadan AEH (2023) Anti-tumor activity of orally administered gefitinib-loaded nanosized cubosomes against colon cancer. *Pharmaceutics* 15(2): 680. <https://doi.org/10.3390/pharmaceutics15020680>
- El-Tanani M, Platt-Higgins A, Lee YF, Al Khatib AO, Haggag Y, Sutherland M, Zhang SD, Aljabali AAA, Mishra V, Serrano-Aroca A,

- Tambuwalla MM, Rudland PS (2022) Matrix metalloproteinase 2 is a target of the RAN-GTP pathway and mediates migration, invasion and metastasis in human breast cancer. *Life Sciences* 310(121046): 121046. <https://doi.org/10.1016/j.lfs.2022.121046>
- Elzayat EM, Sherif AY, Nasr FA, Attwa MW, Alshora DH, Ahmad SF, Alqahtani AS (2023) Enhanced codelivery of gefitinib and azacitidine for treatment of Metastatic-Resistant lung cancer using biodegradable lipid nanoparticles. *Materials* 16(15): 5364. <https://doi.org/10.3390/ma16155364>
- Fois SS, Paliogiannis P, Zinellu A, Fois AG, Cossu A, Palmieri G (2021) Molecular epidemiology of the main druggable genetic alterations in non-small cell lung cancer. *International Journal of Molecular Sciences* 22(2): 612. <https://doi.org/10.3390/ijms22020612>
- Godugu C, Doddapaneni R, Patel AR, Singh R, Mercer R, Singh M (2016) Novel gefitinib formulation with improved oral bioavailability in treatment of A431 skin carcinoma. *Pharmaceutical Research* 33(1): 137–154. <https://doi.org/10.1007/s11095-015-1771-6>
- Golubeva OY, Alikina YA, Brazovskaya EY, Ugolkov VV (2020) Peculiarities of the 5-fluorouracil adsorption on porous aluminosilicates with different morphologies. *Applied Clay Science* 184: 105401. <https://doi.org/10.1016/j.clay.2019.105401>
- Huang Y, Hu QH, Song GX, Tao Z, Xue SF, Zhu QJ, Zhou QD, Wei G (2014) Cucurbit[7,8]urils binding to gefitinib and the effect of complex formation on the solubility and dissolution rate of the drug. *RSC Advances* 4(7): 3348–3354. <https://doi.org/10.1039/c3ra45017a>
- Huang K, Ren C, Lai Z, Yu Y, Dai D (2022) Hyperspectral image classification via discriminant Gabor Ensemble filter. *IEEE Transactions on Cybernetics* 52(8): 8352–8365. <https://doi.org/10.1109/tcyb.2021.3051141>
- Jadus MR, Natividad J, Mai A, Ouyang Y, Lambrecht N, Szabo S, Ge L, Hoa N, Dacosta-Iyer MG (2012) Lung cancer: A classic example of tumor escape and progression while providing opportunities for immunological intervention. *Clinical and Developmental Immunology* 2012: 1–21. [Hindawi Limited] <https://doi.org/10.1155/2012/160724>
- Jakubowski M, Kucinska M, Ratajczak M, Pokora M, Murias M, Voelkel A, Sandomierski M (2022) Zinc forms of faujasite zeolites as a drug delivery system for 6-mercaptopurine. *Microporous and Mesoporous Materials* 343: 112194. <https://doi.org/10.1016/j.micromeso.2022.112194>
- Jesudoss SK, Vijaya JJ, Kaviyarasu K, Kennedy LJ, Jothi Ramalingam R, Al-Lohedan HA (2018) Anti-cancer activity of hierarchical ZSM-5 zeolites synthesized from rice-based waste materials. *RSC Advances* 8(1): 481–490. <https://doi.org/10.1039/c7ra11763a>
- Jiang Z, Li Y, Wei Z, Yuan B, Wang Y, Akakuru OU, Li Y, Li J, Wu A (2021) Pressure-induced amorphous zeolitic imidazole frameworks with reduced toxicity and increased tumor accumulation improves therapeutic efficacy in vivo. *Bioactive Materials* 6(3): 740–748. <https://doi.org/10.1016/j.bioactmat.2020.08.036>
- Johne A, Scheible H, Becker A, Van Lier JJ, Wolna P, Meyring M (2020) Open-label, single-center, phase I trial to investigate the mass balance and absolute bioavailability of the highly selective oral MET inhibitor tepotinib in healthy volunteers. *Investigational New Drugs*, 38(5): 1507–1519. <https://doi.org/10.1007/s10637-020-00926-1>
- Kariminezhad H, Habibi M, Mirzababayi N (2015) Nanosized ZSM-5 will improve photodynamic therapy using Methylene blue. *Journal of Photochemistry and Photobiology B, Biology* 148: 107–112. <https://doi.org/10.1016/j.jphotobiol.2015.03.013>
- Kola Srinivas NS, Verma R, Pai Kulyadi G, Kumar L (2016) A quality by design approach on polymeric nanocarrier delivery of gefitinib: formulation, in vitro, and in vivo characterization. *International Journal of Nanomedicine* 12: 15–28. <https://doi.org/10.2147/ijn.s122729>
- Kutkut M, Shakya AK, Nsairat H, El-Tanani M (2023) Formulation, development, and in vitro evaluation of a nanoliposomal delivery system for mebendazole and gefitinib. *Journal of Applied Pharmaceutical Science* 13(6): 1–14. <https://doi.org/10.7324/japs.2023.110512>
- Li Y, Song F, Cheng L, Qian J, Chen Q (2019) Functionalized large-pore mesoporous silica microparticles for gefitinib and doxorubicin codelivery. *Materials* 12(5): 766. <https://doi.org/10.3390/ma12050766>
- Liao T, Den, J, Chen W, Xu J, Yang G, Zhou M, Zhilei Lv, Wang S, Song S, Tan X, Yin Z, Li Y, Jin Y (2022) Fasudil increased the sensitivity to gefitinib in NSCLC by decreasing intracellular lipid accumulation. *Cancers* 14(19): 4709. <https://doi.org/10.3390/cancers14194709>
- Malam Y, Loizidou M, Seifalian AM (2009) Liposomes and nanoparticles: nanosized vehicles for drug delivery in cancer. *Trends in Pharmacological Sciences* 30(11): 592–599. <https://doi.org/10.1016/j.tips.2009.08.004>
- Martinho O, Vilaça N, Castro PJG, Amorim R, Fonseca AM, Baltazar F, Reis RM, Neves IC (2015) In vitro and in vivo studies of temozolomide loading in zeolite structures as drug delivery systems for glioblastoma. *RSC Advances* 5(36): 28219–28227. <https://doi.org/10.1039/c5ra03871e>
- Mavrodinova V, Popova M, Yoncheva K, Mihály J, Szegedi Á (2015) Solid-state encapsulation of Ag and sulfadiazine on zeolite Y carrier. *Journal of Colloid and Interface Science* 458: 32–38. <https://doi.org/10.1016/j.jcis.2015.07.026>
- Narayan R, Gadag S, Garg S, Nayak UY (2022) Understanding the effect of functionalization on loading capacity and release of drug from mesoporous silica nanoparticles: A computationally driven study. *ACS Omega* 7(10): 8229–8245. <https://doi.org/10.1021/acsomega.1c03618>
- Pandit D, Chadha R, Laha B, Gautam M, Karan M, Mandal SK (2022) Novel pharmaceutical cocrystals of gefitinib: A credible upswing in strategic research to ameliorate its biopharmaceutical challenges. *Crystal Growth & Design* 22(4): 2218–2229. <https://doi.org/10.1021/acs.cgd.1c01328>
- Salehi N, Kuminek G, Al-Gousous J, Sperry DC, Greenwood DN, Waltz NM, Amidon GL, Ziff RM, Amidon GE (2021) Improving dissolution behavior and oral absorption of drugs with pH-dependent solubility using pH modifiers: A physiologically realistic mass transport analysis. *Molecular Pharmaceutics* 18(9): 3326–3341. <https://doi.org/10.1021/acs.molpharmaceut.1c00262>
- Shah A, Patel A, Dharamsi A (2021) Optimization of solid lipid nanoparticles and nanostructured lipidic carriers as promising delivery for gefitinib: characterization and invitro evaluation. *Current Drug Therapy* 16(2): 170–183. <https://doi.org/10.2174/1574885516666210125111945>
- Sherif AY, Harisa GI, Shahba AA, Alanazi FK, Qamar W (2023) Optimization of gefitinib-loaded nanostructured lipid carrier as a biomedical tool in the treatment of metastatic lung cancer. *Molecules (Basel, Switzerland)* 28(1): 448. <https://doi.org/10.3390/molecules28010448>
- Shi J, Zhao G, Teng J, Wang Y, Xie Z (2018) Morphology control of ZSM-5 zeolites and their application in Cracking reaction of C4 olefin. In *Inorganic Chemistry Frontiers* 5(11): 2734–2738. [Royal Society of Chemistry (RSC)] <https://doi.org/10.1039/c8qi00686e>

- Siegel RL, Miller KD, Fuchs HE, Jemal A (2022) Cancer statistics, 2022. *Cancer Journal for Clinicians* 72(1): 7–33. <https://doi.org/10.3322/caac.21708>
- Smith MC, Crist RM, Clogston JD, McNeil SE (2017) Zeta potential: a case study of cationic, anionic, and neutral liposomes. *Analytical and Bioanalytical Chemistry* 409(24): 5779–5787. <https://doi.org/10.1007/s00216-017-0527-z>
- Sun L, Wang Z, Chen L, Yang S, Xie X, Gao M, Zhao B, Si H, Li J, Hua D (2020) Catalytic Fast Pyrolysis of Biomass into Aromatic Hydrocarbons over Mo-Modified ZSM-5 Catalysts. *Catalysts* 10(9): 1051. <https://doi.org/10.3390/catal10091051>
- Yang F, Wen X, Ke QF, Xie XT, Guo YP (2018) pH-responsive mesoporous ZSM-5 zeolites/chitosan core-shell nanodisks loaded with doxorubicin against osteosarcoma. *Materials Science & Engineering, C, Materials for Biological Applications* 85: 142–153. <https://doi.org/10.1016/j.msec.2017.12.024>
- Zaleskis G, Garberyt, S, Pavliukeviciene B, Krasko JA, Skapas M, Talaikis M, Darinskas A, Zibutyte L, Pasukoniene V (2021) Comparative evaluation of cellular uptake of free and liposomal doxorubicin following short term exposure. *Anticancer Research* 41(5): 2363–2370. <https://doi.org/10.21873/anticancerres.15011>
- Zarshenas P (2022) ZSM-5-5-FU as a Drug Delivery Platform for 5-Fu. *Biomedical Journal of Scientific & Technical Research* 43(1): 34216–34220. <https://doi.org/10.26717/bjstr.2022.43.006844>
- Zhai L, Zhang Z, Guo L, Dong H, Yu J, Zhang G (2022) Gefitinib-resveratrol Cocrystal with optimized performance in dissolution and stability. *Journal of Pharmaceutical Sciences* 111(12): 3224–3231. <https://doi.org/10.1016/j.xphs.2022.09.031>
- Zhao H, Li T, Yao C, Gu Z, Liu C, Li J, Yang D (2021) Dual roles of metal-organic frameworks as nanocarriers for miRNA delivery and adjuvants for chemodynamic therapy. *ACS Applied Materials & Interfaces* 13(5): 6034–6042. <https://doi.org/10.1021/acsami.0c21006>